



ELSEVIER

Journal of Chromatography A, 869 (2000) 231–241

JOURNAL OF
CHROMATOGRAPHY A

www.elsevier.com/locate/chroma

Performance of experimental sample injectors for high-performance liquid chromatography microcolumns

Marc D. Foster*, Megan A. Arnold, Jon A. Nichols, Stephen R. Bakalyar

Rheodyne, L.P., P.O. Box 1909, Rohnert Park, CA 94927-1909, USA

Abstract

An experimental injector for HPLC microcolumns and a 3-nl conductivity detector connected directly to the injector outlet with a 19-nl tube were used to study injector dispersion, guide the design of improved injectors, and suggest appropriate injection techniques. With regard to the small injection volumes required when no on-column concentration technique is used, we show that in some circumstances: (i) there are two volumes to be considered, the sample volume (that which is intended to be injected) and the effective injection volume (that which contains all the sample after it has completely emerged from the injector). Due to dispersion, the latter is often many times the former. An injector performance factor is defined as the ratio of the two volumes. (ii) A smaller sample chamber volume in an injector does not necessarily produce a proportionately smaller effective injection volume, in which case there is a reduction of peak height that degrades sensitivity without a commensurate reduction in peak width that would improve resolution. (iii) Adjusting the geometry of the sample chamber and stator passage can significantly improve injector performance, as illustrated for sample volumes from 2 nl to 1 μ l. (iv) In some cases, reducing the diameter of an injector passageway in an attempt to reduce dispersion actually causes performance to worsen. © 2000 Elsevier Science B.V. All rights reserved.

Keywords: Injection techniques; Sample volume; Injector dispersion; Injector performance; Instrumentation

1. Introduction

As the diameters of high-performance liquid chromatography (HPLC) columns are reduced, peaks are eluted in smaller volumes, and there is a more acute need to limit the dispersion (band broadening) caused by extra-column components, in order to prevent degradation of resolution. Recent, general discussions of the unique requirements for micro-column liquid chromatography have been published by several authors [1–7]. The dispersion caused by post-column components, such as detectors, diversion valves and connecting tubing, is in all cases a

concern, so they must be selected carefully. The dispersion caused by pre-column components, such as sample injectors, column selection valves, column switching valves, column inlet filters and connecting tubing, is a concern only under some operating conditions.

When techniques are used that result in on-column concentration (focusing or peak compression), pre-column dispersion is mitigated for all but weakly retained sample components [1,3,8–13]. This is the case when using gradient elution [14,15], when using a trap column [16], or when diluting the sample with weak solvent [12,17]. In such techniques it is common to inject large sample volumes in order to enhance detection sensitivity. Such volumes would in other circumstances produce a wide initial sample

*Corresponding author.

zone, in effect creating a large pre-column dispersion that severely degrades resolution.

The benefits of on-column concentration are not available in simple isocratic operation, so in this technique it is important to minimize dispersion that occurs before the sample enters the column. The subject of this study is injector dispersion under these circumstances. A previous study [12] discussed the effect of sample volume on resolution and detection sensitivity, covering sample volumes from 400 nl to 130 μ l and columns with inside diameters of 1 mm, 2.1 mm and 4.6 mm. That study also discussed the basic theory of extra-column dispersion in general and injector dispersion in particular, and contained a commentary on injection techniques. The present study also deals with sample volume, but delves more deeply into the sources of injector dispersion, and is primarily concerned with smaller injection volumes, between 2 nl and 1 μ l, which are appropriate for column diameters of 50 μ m to 1 mm.

Two experimental approaches provided the novel information in this report. One was the use of a custom-fabricated conductivity detector. The volume of the conductivity cell was 3 nl. The volume of the tube used to connect the cell to the outlet of the injector was 19 nl. The dispersion of this tube-detector combination was extremely small, so that in most cases, when connected directly to the outlet of the injector under study, the observed peak widths could be considered to be due primarily to the injector. A single solute was injected and a single peak observed. The other tactic was the use of an experimental sandwich injector. Its relatively simple architecture let the geometry of the internal flow passages be changed in a systematic way and facilitated theoretical interpretation of the data. Ex-

perimental work was limited to manual sample injection. However, some of the insights apply to injection by an autosampler.

We present a finding of practical significance for the practicing chromatographer regarding injection volumes. A consequence of dispersion in some injector designs is that it is counter productive to reduce beyond a certain volume the size of the sample chamber, in order to scale down the sample to match a small column and thereby maximize resolution. A smaller sample chamber volume in an injector does not necessarily produce a proportionately narrower band, in which case there is a reduction of peak height without a commensurate reduction in peak width. That is, the limit of detection is degraded without gaining any resolution.

Finally, we show that adjusting the geometry of the sample chamber and stator passage can significantly improve injector performance. This finding suggests guidelines for designing improved injectors and for using appropriate injection techniques.

2. Experimental

2.1. Sample volumes

Sample volumes were chosen to be appropriate for various column sizes. Table 1 shows typical sample volumes used for column diameters from nanoscale fused-silica columns to classical analytical scale columns for isocratic operation. The table is divided into an “optimal resolution” case where the achievement of resolution is paramount, requiring a small injection volume, and an “optimal sensitivity” case where larger volumes are injected in order to im-

Table 1
Typical sample volumes

Column I.D.	Area ratio	Flow-rate	Typical sample volume	
			Optimal resolution	Optimal sensitivity
4.6 mm	1	1 ml/min	20 μ l	100 μ l
2.1 mm	0.208	200 μ l/min	4 μ l	20 μ l
1 mm	0.047	50 μ l/min	1 μ l	5 μ l
300 μ m	0.004	4 μ l/min	80 nl	400 nl
180 μ m	0.0015	1.5 μ l/min	30 nl	150 nl
100 μ m	0.00047	500 nl/min	9 nl	45 nl
50 μ m	0.00012	100 nl/min	2 nl	10 nl

prove the limit of detection while accepting somewhat compromised resolution of early peaks. The sample volumes have been derived for the different column diameters by multiplying a 20- μ l injection for isocratic operation of a 4.6-mm column by the column area ratios. Thus all columns within a column of data are loaded with the same volume of sample as a percentage of the total column volume.

Sample volumes for optimal resolution in Table 1, are those below which there is little practical gain in resolution for peaks with $k > 1$, as is the case with the 20- μ l injection into an isocratically operated 150 \times 4.6 mm column packed with 5- μ m particles. Caveat: For a given column diameter, reducing either the column length or the packing particle diameter while maintaining the same flow-rate will result in eluting peak volumes which are narrower than for the case given here. Such columns may show improved resolution by further reducing the sample volume.

Sample volumes for optimal sensitivity in Table 1, are those that compromise resolution but that significantly improve peak height and thus the limit of detection. They are five times the isocratic optimal resolution volumes. Two caveats: (i) volumes can be larger in some cases. As mentioned in the introduction, when techniques are used that result in on-column concentration, pre-column dispersion is mitigated, so when using a trap column or when diluting the sample with weak solvent, much higher

volumes than shown in the table are possible. (ii) Volumes must be smaller in some cases. In instruments which have a significant delay volume before the start of the gradient reaches the column, the early peaks will elute under essentially isocratic conditions, so use of the optimal sensitivity volumes often will cause those peaks to be unacceptably wide.

The volumes in Table 1 are approximate, and have been investigated experimentally in the authors' laboratory as discussed further in Ref. [12], which shows how the resolution, sensitivity and appearance of chromatograms change as a function of sample volume in both isocratic and gradient operation with different column diameters, systems with different extra-column dispersion, and peaks throughout the range of $k = 0$ to 5.

2.2. Sample injectors

Fig. 1 is a diagram of the architecture of the experimental and commercial injectors used in this study. They are sandwich injection valves that comprise a flat rotor sandwiched between two flat stators. This commercial model has been available since 1983. Similar sandwich type valve architectures have been described by other authors [18,19]. The rotor contains the sample chamber, a straight passage that, in the INJECT position, aligns coaxially with a straight stator passage that connects

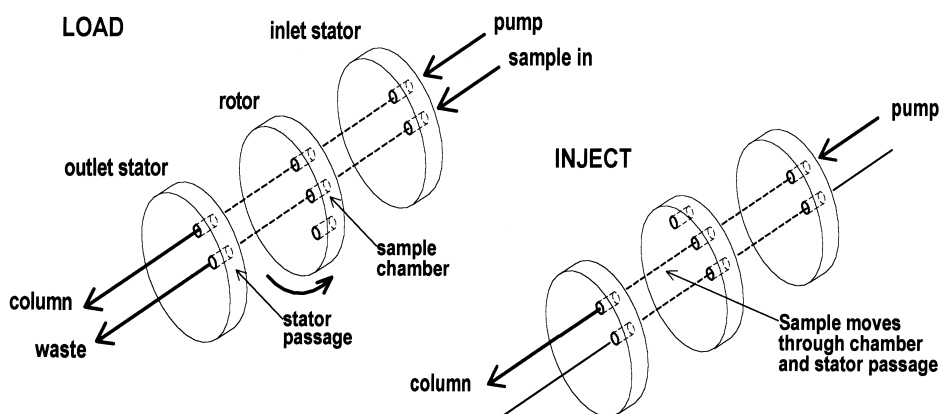


Fig. 1. Architecture of the sandwich injectors studied. The Rheodyne Model 7520 and experimental versions of it is useful for studying the mechanisms of injector dispersion because it has a relatively simple architecture. The three parts are aligned with a common center pin that assists in aligning the sample chamber with the outlet stator passage in the INJECT position. With complete-fill injections, dispersion takes place in both the sample chamber and the outlet stator passage (see Fig. 2). With timed injections, dispersion is only in the outlet stator passage.

the sample chamber to the column-attachment tube or, in the case of most of the experiments, to the inlet tube of the micro conductivity detector. When using the complete-fill technique of injection (the chamber is completely filled with sample), the sample volumes were varied by changing the diameters and lengths of the chambers.

Two chamber lengths were used, 2 mm and 6.9 mm. For sample volumes of 200, 500 and 1000 nl, with chamber lengths of 6.9 mm, the injectors are commercially available versions of the Rheodyne Model 7520 Internal Sample Chamber Micro-Scale Injector (Rheodyne, Rohnert Park, CA, USA). These sample chambers have inner diameters of 0.2, 0.3 and 0.43 mm, respectively. Smaller volume versions of the 6.9 mm long chambers were created by filling the 0.3-mm hole with a section of a fused-silica capillary tube with dimensions given in Fig. 5. The 2-mm long sample chambers are experimental variations of the commercial model with sample volumes of 25, 65, 150 and 290 nl.

Outlet stators having two different diameters were used in this study. The standard stator of 127 μm I.D. was used as well as a special 25 μm I.D. stator passage. The 25- μm I.D. stator passage was created by filling the standard stator with a short section of 120 μm O.D. \times 25 μm I.D. fused-silica.

2.3. Column

The column was 150 mm \times 300 μm , Hypersil C₁₈ BDS, 3 μm particle size (LC Packings, San Francisco, CA, USA).

2.4. Instrumentation

The conductivity detector was custom made. It had a 3-nl detection cell, constructed by drilling a 127- μm hole through two 75- μm thick pieces of brass, between which was sandwiched a 75- μm thick Kapton spacer. The cell was connected to the outlet stator of the injector with a 39 mm \times 25 μm I.D. tube containing 19 nl. A Wescan conductivity meter was used to drive and measure the conductivity signal. The drive signal was about 40 Hz.

The UV detector was a Model HP 1100 (Hewlett-Packard, Little Falls, PA, USA) with a 3-nl flow cell,

Model UZ-HP11-NAN (LC Packings), connected by 20- μm I.D. tubing.

The pump was an Eldex MicroPro syringe pump (Eldex, Napa, CA, USA).

2.5. Chemicals

HPLC-grade water (EM Science, Gibbstown, NJ, USA) was the mobile phase when the micro conductivity detector was connected directly to the injector. For column experiments this water was mixed with acetonitrile (Aldrich, Milwaukee, WI, USA) to form an acetonitrile–water (60:40) mobile phase. The sample for the experiments using the conductivity detector and no column was sodium nitrate (J.T. Baker, Phillipsburg, NJ, USA). The sample for the experiments using the UV detector and a column consisted of uracil, benzyl alcohol, phenethyl alcohol, acetophenone, propiophenone, butyrophenone, valerophenone and hexanophenone (Aldrich) dissolved in the mobile phase. The alkylphenones were purified using preparative chromatography on a 10-mm I.D. C₁₈ column.

3. Results and discussion

3.1. Definition of effective injection volume and injector performance

The following terms in italics are defined. Injector performance is determined by connecting a micro detector directly to the injector and monitoring the emerging *injector peak*. The width and shape of this peak, indicating the *injector dispersion*, is governed by the geometry of the passages through which sample flows during the injection process and the technique used to load the injector. This applies to both manual injectors and autosamplers.

We distinguish between the volume the user selects and the volume that emerges from the injector. The *sample volume*, V_s , is that intended to be injected, such as when 1- μl is dispensed from a syringe into a sample chamber in the partial-filling technique, or when several microliters are loaded into a 1- μl sample chamber in the complete-filling technique. The *effective injection volume*, V_e , is that containing the peak after it has completely emerged

from the injector. V_e is larger than V_s , due to dispersion. For a Gaussian peak, V_e is the volume containing four standard deviations, 4σ (μl). However, injector peaks are typically asymmetric, so we must use other means to characterize them. We can define V_e as the volume between the start and end of the peak. In the data reported here, the start and end of the peak was defined as the point at which the signal crosses 13% of peak maximum.

The *injector performance*, $P_{i,w}$, is the ratio of these two peak width volumes.

$$P_{i,w} = \frac{V_s}{V_e} \quad (1)$$

We can also define injector performance in terms of the variance, σ^2 , in μl^2 , of the two volumes. Variances are determined by central statistical moment calculations of the concentration profile. They apply to peaks of any shape [20]. We can consider the ideal sample volume to be a “plug” of uniform concentration. Scanning the sample chamber from one end to the other, the concentration profile would be a rectangular peak. A perfect injector would have no dispersion, producing an effective injection volume that was an undistorted replica of the plug. This would result, for example, if a sample chamber was filled completely with sample of uniform concentration and if, during travel of the sample out of the injector, (i) the plug’s front boundary did not disperse as it passed through the channels of the injector stator, and (ii) the plug’s rear boundary did not disperse as it passed through the sample chamber and through the channels of the injector stator. The central statistical moment of such a rectangular profile is the square of the volume (width of the peak), the quantity divided by 12. The variance-

based injector performance, $P_{i,v}$, can then be defined as a ratio of the two variances, as an alternative to Eq. (1).

$$P_{i,v} = \sqrt{\frac{\sigma_{\text{plug}}^2}{\sigma_e^2}} = \sqrt{\frac{V_s^2/12}{\sigma_e^2}} \quad (2)$$

Using either equation, a perfect injector has a performance factor of 1. The injectors in this study had performance ranging from 0.04 to 0.6, when used in the complete-fill mode.

3.2. Expected dispersion within a sandwich injector

From the above discussion, we can expect injection peaks in the complete-fill mode to be asymmetric, since the plug’s front boundary does not have to pass through the sample chamber, whereas the rear boundary necessarily disperses as it passes through the chamber. Fig. 2 is a scale drawing of one of the injectors studied, showing the relative proportions of the lengths and diameters of the sample chamber and stator passage. The shadings give a qualitative description of laminar flow through the valve to illustrate how the valve works. It was chosen because it illustrates the various dispersion mechanisms that can take place. It shows three stages of injection: Fig. 2A shows the completely filled sample chamber prior to injection. The profile of this sample is a square peak. Fig. 2B shows the state of the sample as it begins to be displaced from the sample chamber. The injection peak front disperses in the stator passage, while the rear disperses in the sample chamber. In this example, the magnitude of dispersion, expressed as variance, for the

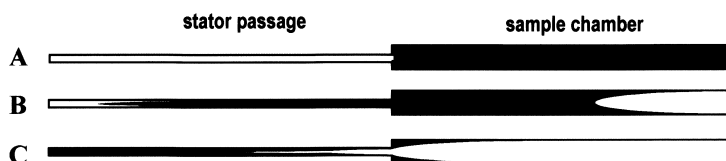
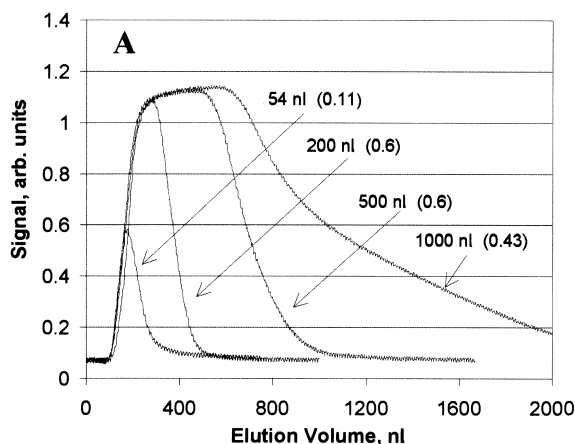


Fig. 2. Dispersion of peak front and peak rear in a sandwich injector. This is a scale drawing of the injector flow passages in one of the injectors studied. The $1\text{-}\mu\text{l}$ sample chamber has dimensions of $6.9\text{ mm long} \times 430\text{ }\mu\text{m diameter}$. The outlet stator passage has dimensions of $6.9\text{ mm long} \times 127\text{ }\mu\text{m diameter}$. The three views are: (A) prior to injection the sample chamber is completely filled. (B) Shortly after the chamber is rotated to the INJECT position. The peak front disperses only in the stator. The peak rear disperses in the chamber. (C) After additional time. Dispersion of the peak rear is large because of the large chamber diameter, and because of the poor convection at the chamber–stator boundary of the mismatched passage diameters.

peak front will be less than the peak rear, due to the high dependence of dispersion on passage diameter. The parabolic profile of the flow velocity is reflected in the shape of the sample–mobile phase boundaries. For the sake of illustration, these boundaries are shown as distinct, whereas they are in reality diffuse. Also, the distance traveled in the sample chamber has been exaggerated compared to the distance in the stator passage. Fig. 2C shows a later state, when most of the sample has been displaced from the chamber, and the peak rear is experiencing two distinct dispersion mechanisms. It is being dispersed as it passes through the stator passage. And, because of the poor longitudinal convection at the end of the sample chamber due to the large mismatch in diameters, a significant amount of sample lingers at the chamber wall, and can be expected to produce a high degree of dispersion manifested as a change in the slope (tail) of the peak rear. This behavior is in fact experimentally observed, as discussed below. It should be noted that these are strictly qualitative descriptions of what may occur in the valve passage. An exact model is beyond the scope of this text.

3.3. Observed dispersion with large sample chamber diameters and a 6.9-mm long chamber

Fig. 3A shows the injection peaks from sample chambers of 54, 200, 500 and 1000 nl operated in the



complete-fill mode at 1 $\mu\text{l}/\text{min}$, with a 127 μm diameter stator passage. The following observations are made when considering the injection peak shapes from left to right. The calculated injector performance for each sample chamber, $P_{i,w}$, is listed in parentheses.

The 100-nl delay before the peak onset is caused by the volume of the stator passage (87 nl) plus the volume of the tube connecting to the detector (19 nl).

All four peak fronts have the same dispersion (slope) because they all experience the same stator passage and do not experience the sample chambers.

For the larger volumes, the nearly constant concentration is observed for a portion of the peak. This is the part where nearly all dispersion of the peak front has cleared the detector, and the beginning of the dispersion of the peak rear is yet to reach the detector. The variances of the larger sample volume plugs tend to dominate the dispersion in the stator, and the peaks start to approach the rectangular shape of an ideal injection.

Looking at the top half of the peaks, for the 500- and 1000-nl volumes, the peak rears have a lower slope (higher dispersion) than the fronts, since they experience both the sample chamber and the stator passage. It is not clear why the peak rears of the smaller volumes do not show a greater dispersion.

Looking at the bottom half of the peaks, for the

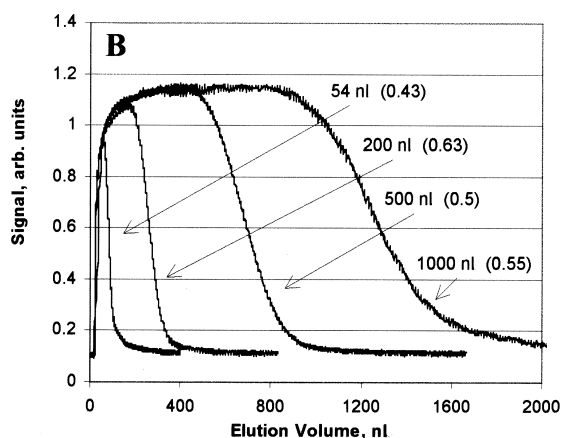


Fig. 3. Observed dispersion with large sample chamber diameters and a 6.9-mm long chamber. The sample chamber and outlet stator passages are both 6.9 mm long. In (A) the “standard” stator passage diameter is 127 μm . In (B) the experimental “reduced bore” stator passage diameter is 25 μm . Sample chamber volumes and (diameters) are 1000 nl (430 μm), 500 nl (300 μm), 200 nl (200 μm) and 54 nl (100 μm). The injector performance at each sample volume, $P_{i,w}$, is shown in parentheses. See text for a discussion of the peak shapes.

500-nl and especially the 1000-nl volumes, dispersion is very high, presumably due to the poor convection mechanism discussed above for the highly mismatched diameters of the sample chamber and the stator passage. Noting the performance numbers, we see that, for this architecture with this stator, the best performance is achieved for the mid-range volumes.

The 54-nl peak illustrates that going to smaller sample volumes does not necessarily provide a proportional decrease in peak width. Dropping from a sample volume of 200-nl to one of 54-nl ($54/200=0.27$) does not result in a peak that is proportionately narrower, i.e., 27% as wide. The width reduction went down to only about 50%. The injector performance dropped from ~ 0.6 to ~ 0.1 . This is because the dispersion of the outlet stator passage becomes increasingly significant compared to the plug dispersion as sample volume is reduced. Further reductions in sample volume reduce the effective injection volume very little. This aspect of injector performance is further illustrated in the next section.

Caveat: This data is for only one flow-rate. Peak profiles are different at other flow-rates (data not shown). In general, the dispersion for any given design increases with increased flow-rate.

Fig. 3B shows the injection peaks from the same sample chambers as Fig. 3A, but using a stator passage diameter reduced from 127 μm to 25 μm , producing a stator passage volume of ~ 3 nl.

The delay before the peak onset is now reduced to 20 nl.

Again, all four peak fronts have the same slope, but it is, as expected, higher (lower dispersion) due to the smaller outlet stator passage.

The dispersion of the peak rears has improved only slightly, indicating the dominance of the chamber dispersion.

The performance of the 54-nl sample is improved.

3.4. Observed loss of performance with decreasing sample volumes

3.4.1. Observations of injection peaks

Reducing the sample volume does not necessarily reduce proportionately the effective injection volume, and as a consequence, the peak height is

reduced without a commensurate reduction in peak width (improvement in resolution). The detector was connected directly to the injector as before. Different volume injections were made of 16, 8, 4, 2 and 1 nl. The corresponding effective injection volumes are 137, 123, 117, 115 and 115 nl. For this architecture, with this stator passage diameter, smaller sample volumes do not necessarily result in significantly narrower peaks. The effective injection volumes reach a limit at about 115 nl. This is because the dispersion in the stator passage becomes large compared to the sample plug variance of very small sample volumes. Another way of illustrating the diminishing returns of continually reducing sample volume is to calculate the injector performance numbers from Eq. (1). They decrease from ~ 0.1 for the 16-nl sample to ~ 0.01 for the 1-nl sample.

These small sample volumes were created by using the timed injection technique (also termed temporary, moving and time slice injection), that has been reviewed in Ref. [12]. If the dispersion in the stator passage is very small compared to the volume of the sample, the timed injection technique results in an injection peak with a profile that is nearly perfect, i.e., a rectangular peak profile and an injector performance of close to 1. However, with very small injection volumes, as in this case, the dispersion of the stator passage significantly distorts this plug.

Timed injection works as follows. After completely filling the sample chamber so that the concentration is a uniform 100% throughout, the injector is switched to the INJECT position and left there only long enough for the mobile phase to transfer the desired volume out of the loop ($s \times \mu\text{l}/s = \mu\text{l}$ injected). The dispersion in the chamber must be such that, at the time that the injector is returned to LOAD, sample emerging from the chamber is still at the initial concentration, i.e., the dispersing peak rear does not reach the stator passage before the chamber is cut off line.

3.4.2. Observations of chromatographic resolution

Fig. 4 is a series of chromatograms using a 150 mm \times 300 μm , 3 μm column. Sample was introduced by temporary injections. The resolution of peaks 2 and 3 improves as sample volume is decreased, but not below 200 nl. The effective injection volumes are shown; they were determined

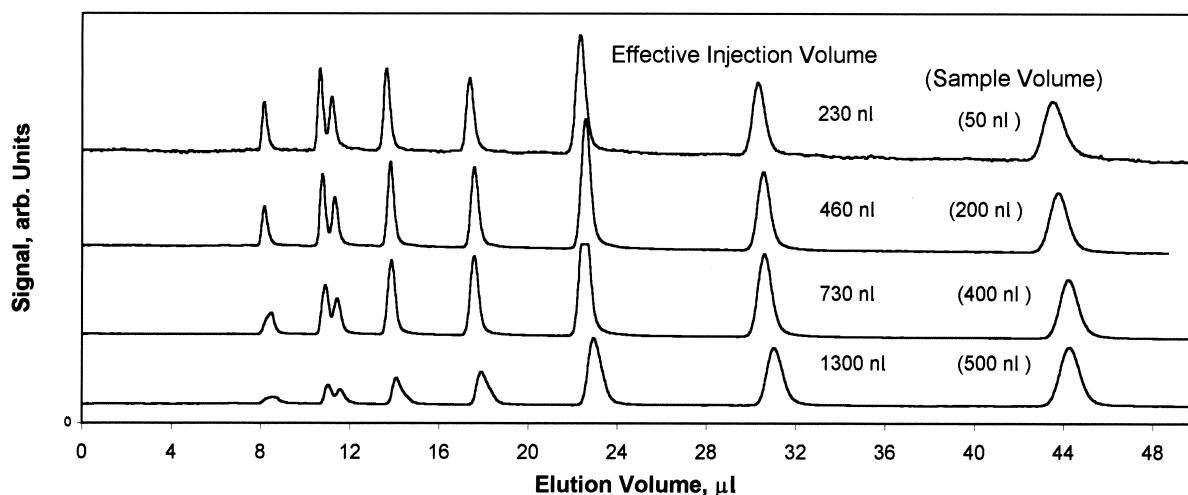


Fig. 4. Trade off between resolution and detection sensitivity on a microcolumn in isocratic operation. The resolution of peaks 2 and 3 can be quantified as a ratio between the height of the valley between them and the height of peak 3. Starting at a 500-nl sample volume (ratio is 0.7) the resolution is improved with the next two lower volumes (ratio is 0.5 and 0.3). However, the 50-nl sample volume is seen not to be an improvement over the 200-nl volume, illustrating that reducing sample volume beyond a certain point does not always gain resolution. In this case, going from 200 nl to 50 nl reduces the limit of detection by a factor of four, and gains nothing in resolution. Timed injection was used (see text) to achieve the different sample volumes. The same sample was used in each case but the signal height has been adjusted so that peak 8 is the same height for each chromatogram, in order to show the relative height differences of the earlier peaks. Column: 150 mm \times 300 μ m, 3 μ m C_{18} . Mobile phase: acetonitrile–water (60:40). Flow-rate: 3 μ l/min. Detector: 3-nl UV flow cell operated at 250 nm and an attenuation of 15.63 mAU/V. All peaks were less than 15 mAU in height. Compounds are, in order, uracil (unretained), benzyl alcohol, phenethyl alcohol, acetophenone, propiophenone, butyrophenone, valerophenone and hexaphenone.

by connecting a detector directly to the injector (data not shown). Although the effective injection volume for the 50-nl sample volume is in fact lower than that for the 200-nl sample volume, the difference is small compared to the other sources of dispersion in the system, so an improvement in peak width is not manifested. This behavior is identical to that reported for larger columns [12].

3.5. Observed dispersion with small sample chamber diameters and a 2-mm long chamber

Experimental versions of the commercial 7520 were tested having 2-mm long sample chambers. Inner diameters of the sample chambers were approximately 0.13, 0.2, 0.3 and 0.43 mm producing sample volumes of 25, 65, 150 and 290 nl. The following observations are made.

For the 127- μ m diameter stator passage, the same comments can be made, as in Fig. 3A; however, the dispersion of peaks of roughly corresponding volumes is worse. This is presumably because the

aspect ratio of the sample chambers here is half as large. The classical theory of dispersion in open tubes [21,22] predicts that dispersion (variance) is proportional to the fourth power of the diameter, although more recent theory [23] predicts a somewhat smaller variance for short tubes. In any case, considering only dispersion, the sample chamber should have as small a diameter as possible. Limitations of design, fabrication capability and robustness (immunity to plugging) require some compromises.

For the 25- μ m diameter stator passage, some of the same comments hold as are made in Fig. 3B. However, the reduced diameter of the stator passage improves the injector performance over that of the 127- μ m diameter stator passage, for only the 25-nl sample chamber. For the larger chambers the reduced stator passage diameter degrades performance, especially for the 290-nl chamber. Although the smaller diameter reduces the stator passage dispersion, the dispersion caused by the larger mismatch between chamber and stator passage diameters appears to be large, and results in a net loss of

performance. This illustrates that the absolute volume and geometry of passages through which sample zones pass do not by themselves predict the dispersion of the system. Rather, the relationship of the passage geometry to adjoining fluid elements must also be considered.

3.6. Injection of nanoscale sample volumes

Fig. 5A shows injection peaks for very small sample volumes made from complete-fill injections from sample chambers of 2, 14, 30 and 54 nl. As in Fig. 3A, all peak fronts manifest the same dispersion (slope), and the peak rears have dispersion that is larger than the peak fronts, since they pass through the sample chamber. Injector performance decreased from 0.5 for the 54-nl sample volume to 0.1 for the 2-nl sample volume.

In Fig. 5B the sample volumes were made by timed injection and are so small that the experimental system is unable to accurately report the injector dispersion. Even though the sample chamber makes no contribution to dispersion, and even though the stator passage is small, the dispersion caused by the stator passage, and by the detector and its connecting tube, is significant relative to the plug variance. So the observed effective injection volumes are much larger than the sample volumes, the injector per-

formance ranging from ~ 0.2 for the largest peak to ~ 0.06 for the smallest peak.

4. Conclusions

When micro HPLC columns are used under conditions that do not result in on-column concentration, as in ordinary isocratic operation without the technique of sample dilution with a weak solvent, it is necessary to use small sample volumes to achieve the narrow initial sample zones required for good resolution. The operative volume in such cases is not the sample volume that is loaded into the injector, but the volume that contains all of the sample after it has completely emerged from the injector, which we have called the effective injection volume. Due to dispersion the latter is often many times the former. A measure of an injector's efficiency in producing small effective injection volumes is what we have defined as the injector performance, the ratio of sample volume to effective injection volume. An injector performance of 1 represents ideal behavior. In practice, performance values are much less than this.

This study used an experimental micro sandwich injector, capable of sample volumes from 2 nl to 1 μl , in which the dimensions of both the sample chambers and the outlet stator passages could be

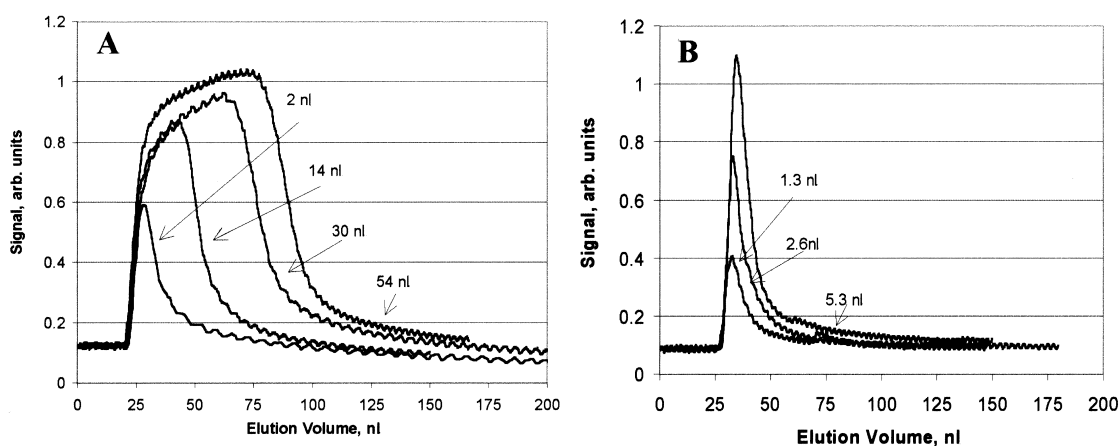


Fig. 5. Injection of nanoscale sample volumes. In (A) the sample chambers of 2, 14, 30 and 54 nl have a length of 6.9 mm and diameters of 25, 50, 75 and 100 μm I.D., respectively. In (B) the sample volumes are made by timed injection, using a chamber 6.9 mm long \times 300 μm in diameter. The stator passage diameter is 25 μm in both figures. A high-speed pneumatic actuator was used to achieve the timed injections.

varied, allowing exploration of some of the design issues in creating high-performance, and providing insight into choosing appropriate injection technique. Although the relatively simple architecture of this injector differs from that found in many manual injectors and autosamplers, some of the important dispersion phenomena that can be investigated are the same ones that occur in other designs. These include dispersion as a function of (i) the diameter of sample chambers and passages connecting the chambers to the rest of the system, (ii) the mismatch of diameters when two passages connect with one another, and (iii) the asymmetry inherent in injection peaks due to the fact that, during injection, the front of the initial sample zone (plug) does not pass through all of the passages experienced by the rear of the sample zone. Not reported in this study are dispersion mechanisms when sample is partially loaded into a chamber flowing in one direction and injected flowing in the opposite direction, as in many front-loading designs and probe-in-loop autosampler designs, and when sample travels through highly curved passages, as in a tightly coiled sample loop, serpentine passage, or passage with a right-angle turn.

A finding useful to practicing chromatographers is that a smaller sample chamber, containing the volume intended to be injected by the complete-fill method, does not necessarily produce a proportionately smaller effective injection volume. When this is the case, it is counterproductive to reduce sample volume below a certain level, in an attempt to improve resolution. The smaller injected sample mass produces a smaller peak height, degrading the limit of detection, without a commensurate reduction in peak width. The volume at which this point is reached depends on the injector used and the dispersion characteristics of the rest of the system, and is best determined experimentally.

This phenomenon of diminishing performance returns can also occur in timed injection, a technique where the dispersion of the sample chamber can be eliminated by returning to the LOAD position before any of the dispersed rear boundary of the sample starts to emerge from the sample chamber. The perfectly shaped rectangular peak that emerges from the chamber necessarily undergoes dispersion as it passes through the injector's outlet stator passage, and,

most significantly, continues to disperse as it travels through the connecting tubing, column and detector. If this extra-chamber dispersion is large relative to the variance of the perfect sample plug, reducing the sample volume below a certain point results in no observable improvement in resolution, the only result being a needless degrading of sensitivity.

A finding useful to instrument designers is that adjusting the geometry of the sample chamber and stator passage can significantly improve injector performance. In general, it is desirable to reduce the diameters of passages through which sample flows on its way out of the injector and to the column. However, the volume and geometry of a passage do not by themselves predict the dispersion contributed to the system. The relationship of the passage geometry to adjoining fluid elements must also be considered. In some circumstances, reducing the diameter of a passage can increase the diameter mismatch to an extent that a smaller passage causes significantly increased dispersion.

References

- [1] J.P.C. Vissers, A.H. de Ru, M. Ursem, J.P. Chervet, *J. Chromatogr. A* 746 (1996) 1.
- [2] R.C. Simpson, *J. Chromatogr. A* 691 (1995) 163.
- [3] J.P. Chervet, M. Ursem, J.P. Salzmann, *Anal. Chem.* 68 (1996) 1507.
- [4] J. Abian, A.J. Oosterkamp, E. Gelpí, *J. Mass Spectrom.* 34 (1999) 244.
- [5] S. Héron, A. Tchaplá, *J. Chromatogr. A* 848 (1999) 95.
- [6] A.P. Köhne, T. Welsch, *J. Chromatogr. A* 845 (1999) 463.
- [7] W.M.A. Niessen, *J. Chromatogr. A* 794 (1998) 407.
- [8] B. Malvasi, V. Ascalone, *J. High Resolut. Chromatogr.* 19 (1996) 503.
- [9] M.A. Rezai, G. Famigliani, A. Capiello, *J. Chromatogr. A* 742 (1996) 69.
- [10] M.J. Mills, J. Maltas, W.J. Lough, *J. Chromatogr. A* 759 (1997) 1.
- [11] C.H. Kientz, A. Verwiej, G.J. de Jong, U.A.Th. Brinkman, *J. Microcol. Sep.* 4 (1992) 477.
- [12] S.R. Bakalyar, C. Phipps, B. Spruce, K. Olsen, *J. Chromatogr. A* 762 (1997) 167.
- [13] J.P. Chervet, R.E.J. van Soest, J.P. Salzmann, *LC·GC Int.* 5 (1992) 33.
- [14] E.C. Huang, J.D. Henion, *J. Am. Soc. Mass Spectrom.* 1 (1989) 158.
- [15] M.T. Davis, T.D. Lee, *Protein Sci.* 1 (1992) 935.
- [16] E.A. Hogendoorn, P. van Zoonen, *J. Chromatogr. A* 703 (1995) 149.

- [17] K. Slais, D. Kourilova, M.R. Gould, J.E. Dickinson, G.A. Desotelle, J. Liq. Chromatogr. 7 (1984) 559.
- [18] T. Takeuchi, D. Ishii, J. High Resolut. Chromatogr., Chromatogr. Commun. 4 (1981) 469.
- [19] A.J.J. Debets, K.-P. Hupe, U.A.Th. Brinkman, W.Th. Kok, Chromatographia 29 (1990) 217.
- [20] J.C. Sternberg, Adv. Chromatogr. 2 (1966) 205.
- [21] G.I. Taylor, Proc. Royal Soc. London A 225 (1956) 67.
- [22] M.J.E. Golay, in: D.H. Desty (Ed.), Gas Chromatography 1958 (Amsterdam Symposium), Butterworths, London, 1958, p. 36.
- [23] M.J.E. Golay, J. Atwood, J. Chromatogr. 186 (1979) 353.